Experimental and theoretical studies of cylindrical Hall thrusters[a)]

Artem Smirnov,[b)] Yegeny Raitses, and Nathaniel J. Fisch

Princeton University Plasma Physics Laboratory, P.O. Box 451, Princeton, New Jersey 08543

The Hall thruster is a mature electric propulsion device that holds considerable promise in terms of the propellant saving potential. The annular design of the conventional Hall thruster, however, does not naturally scale to low power. The efficiency tends to be lower and the lifetime issues are more aggravated. Cylindrical geometry Hall thrusters have lower surface-to-volume ratio than conventional thrusters and, thus, seem to be more promising for scaling down. The cylindrical Hall thruster (CHT) is fundamentally different from the conventional design in the way the electrons are confined and the ion space charge is neutralized. The performances of both the large (9-cm channel diameter, 600–1000 W) and miniaturized (2.6-cm channel diameter, 50–300 W) CHTs are comparable with those of the state-of-the-art conventional (annular) design Hall thrusters of similar sizes. A comprehensive experimental and theoretical study of the CHT physics has been conducted, addressing the questions of electron cross-field transport, propellant ionization, plasma-wall interaction, and formation of the electron distribution function. Probe measurements in the harsh plasma environment of the microthruster were performed. Several interesting effects, such as the unusually high ionization efficiency and enhanced electron transport, were observed. Kinetic simulations suggest the existence of the strong fluctuation-enhanced electron diffusion and predict the non-Maxwellian shape of the electron distribution function. Through the acquired understanding of the new physics, ways for further optimization of this means for low-power space propulsion are suggested. Substantial flexibility in the magnetic field configuration of the CHT is the key tool in achieving the high-efficiency operation. © *2007 American Institute of Physics.*
[DOI: 10.1063/1.2718522]

I. INTRODUCTION

The Hall thruster (HT) is a plasma propulsion device that generates thrust by expelling an accelerated, neutralized ion flux out of the $\mathbf{E} \times \mathbf{B}$ plasma discharge with a closed electron drift.[1–3] In a conventional Hall thruster, the plasma discharge is sustained in the axial electric ($\mathbf{E}$) and radial magnetic ($\mathbf{B}$) fields applied in an annular channel. The magnetic field is large enough to lock the electrons in the azimuthal $\mathbf{E} \times \mathbf{B}$ drift, but small enough to leave the ion trajectories unaffected. The cross-field diffusion of electrons emitted by an external cathode provides the necessary current to sustain the discharge. Ions are accelerated electrostatically in a quasineutral plasma, so that no space-charge limitation is imposed on the achievable current and thrust densities. Existing Hall thrusters can efficiently accelerate a plasma jet to 10–30 km/s (Refs. 4 and 5), while the exhaust velocity in conventional chemical rockets used for space applications typically does not exceed 3 km/s (Ref. 4). Thus, the main advantage offered by plasma propulsion devices, and Hall thrusters in particular, is the significant propellant mass saving, which entails substantial reduction of the launch cost.[6] Alternatively, propellant mass saving allows to accommodate additional scientific instruments aboard the spacecraft. Hall thrusters can be used in space for a variety of low-thrust functions such as satellite orbit control, repositioning, and primary propulsion of relatively lightweight

spacecraft. Conventional design, state-of-the-art Hall thrusters operate at the input power range from subkilowatt to tens of kilowatts with 50%–60% efficiency.

Miniaturized propulsion devices capable of operating in the input power range from hundreds of watts down to a few watts and delivering very low-thrust values (millinewtons and below) will enable a new class of space missions, in which scientific or commercial payload will be distributed among multiple microspacecraft flying in constellations.[7,8] Constellation missions seem attractive for the purposes of high-resolution Earth observations,[9] disaster monitoring,[10] environmental, navigation, and communication services,[10] and magnetic field mapping around the Earth and other planets.[11] The Hall thruster is a mature electric propulsion device at intermediate to high power (hundreds of watts to tens of kilowatts), but it appears promising also for scaling to low-power levels.

In scaling of Hall thrusters to low operating power, the invariance of propellant ionization efficiency requires the thruster channel size to be decreased, while the invariance of the magnetic insulation of the discharge implies that the magnetic field must be increased inversely to the scaling factor.[2,12] Increasing the magnetic field while the thruster channel dimensions are being reduced is challenging because of magnetic saturation in the miniaturized inner parts of the magnetic iron core. Linear scaling down of the magnetic circuit leaves no room for magnetic poles or for heat shields, making difficult the achievement of the optimal magnetic fields. Nonoptimal fields result in enhanced electron trans-

port, power, and ion losses, which lower the efficiency and result in increased heating and erosion of the thruster parts, particularly the critical inner parts of the coaxial channel and magnetic circuit. The major lifetime-limiting process for a Hall thruster is the channel wall sputtering by accelerated ions.[2] The thruster lifetime is reciprocal to the wall erosion rate, which, in turn, is proportional to the power loss per unit area of the wall.[13] Thus, the lifetime of a miniaturized thruster decreases linearly with the scaling parameter and the critical inner parts of the annular channel and magnetic circuit are expected to suffer the largest erosion rates. To avoid enhanced channel erosion is one of the major challenges for low-power Hall thruster technology.

Currently existing low-power Hall thruster laboratory prototypes with channel diameters 2–4 cm operate at 100–200 W power levels with efficiencies in the range of 10–40% (Ref. [6]). However, further scaling of the conventional geometry Hall thruster down to subcentimeter size results in even lower efficiencies, 6% at the power level of about 100 W (Ref. [14]). The low efficiency might arise from a large axial electron current, enhanced by magnetic field degradation due to excessive heating of the thruster magnets, or from a low degree of propellant ionization. Thus, miniaturizing the conventional annular Hall thruster does not appear to be straightforward.

A cylindrical Hall thruster[15] (Fig. [1]), which was proposed by Raitses and Fisch at Princeton Plasma Physics Laboratory (PPPL), overcomes these miniaturization problems. The cylindrical Hall thruster (CHT) has been studied both experimentally and theoretically.[15–22] The principle of operation of the cylindrical Hall thruster is in many ways similar to that of a conventional coaxial Hall thruster, i.e., it is based on a closed $\mathbf{E} \times \mathbf{B}$ electron drift in a quasineutral plasma with magnetized electrons. However, both the forces on the unmagnetized ions, and the means by which the electron drifts close, are quite different, which leads to a profoundly different operation.

The cylindrical thruster consists of a cylindrical ceramic channel, a ring-shaped anode, which serves also as a gas distributor, a magnetic core, and two electromagnetic coils. As compared to the conventional geometry Hall thrusters, the central magnetic pole and the channel piece in the cylindrical thruster are cut down so that the channel has naturally larger volume-to-surface ratio. The electron transport to the anode is suppressed by the mostly radial magnetic field in the annular part of the channel and by the mirror-like magnetic field in the cylindrical part of the channel. The electron drifts are closed and the magnetic field lines form equipotential surfaces, with $\mathbf{E} = -\mathbf{V_e} \times \mathbf{B}$, where $\mathbf{E}$ is the electric field, $\mathbf{B}$ is the magnetic field, and $\mathbf{V_e}$ is the electron drift.

Note that unlike the end-Hall thruster,[23] which has purely cylindrical geometry and biased channel walls, the cylindrical thruster has a ceramic channel with a short annular part to sustain ionization and enable magnetic field configuration with a relatively strong radial component. The length of the annular part of the channel is approximately equal to the ionization mean free path, thus localizing the ionization of the working gas at the boundary of the annular and the cylindrical regions. Hence, most of the voltage drop
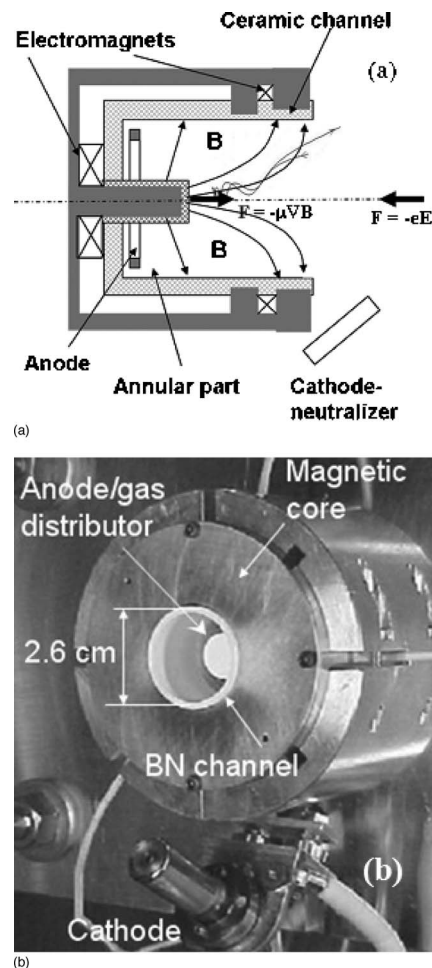

FIG. 1. (a) Schematic of a cylindrical Hall thruster. (b) The 2.6-cm cylindrical Hall thruster.

occurs in the cylindrical region that has large volume-to-surface ratio. Ions are accelerated by the electric field primarily in the direction perpendicular to the magnetic field surfaces, away from the channel walls. In contrast to the conventional (annular) design thruster, due to the absence of inner thruster elements there are no power or ion losses at the inner wall. Higher propellant and current utilization efficiencies should therefore be obtainable. Also, reduced erosion of the inner parts of the channel and magnetic circuit should lead to an increased thruster lifetime, which is particularly critical for the low-power thrusters.

The cylindrical thruster geometry is fundamentally different from the conventional configuration in the way the electrons are confined in the discharge and the ion space charge is neutralized. Electrons in the cylindrical part of the channel are trapped axially in a hybrid magnetoelectrostatic trap: On the anode side, the electrons are impeded from entering the annular part of the channel by the magnetic mirror (see the typical electron trajectory in Fig. [1]), while on the cathode side they are reflected back into the channel by the potential drop in the plume, which is established due to plasma expansion. Therefore, electrons neutralize the ion space charge not by being held axially by the radial magnetic field, as in the conventional thruster. Rather, electrons are

allowed to oscillate axially back and forth, while being trapped axially in the hybrid trap. Thus, one of the fundamental constraints of the conventional thruster configuration is loosened, and the associated physics of this new thruster is quite different. The experiments showed that in virtually all aspects of thruster physics, such as electron transport, ionization of neutrals, potential distribution, etc., the cylindrical thruster exhibits new interesting properties.

Both the large (9-cm channel diameter, 600–1000 W input power) and miniaturized (2.6-cm channel diameter, 50–300 W) CHTs (Refs. 15 and 20) exhibit performances comparable with those of the state-of-the-art conventional (annular) design Hall thrusters of similar sizes. A comprehensive experimental and theoretical study of the CHT physics was conducted, addressing the questions of electron cross-field transport, propellant ionization, plasma-wall interaction, and formation of the electron distribution function.[22] Several interesting phenomena were observed, such as, for example, the unusually high ionization efficiency of the cylindrical thruster and the enhanced electron transport across the magnetic field. The effect of the magnetic field on the thruster discharge was experimentally investigated and the thruster performance was enhanced by optimizing the discharge parameters and the magnetic field configuration. The experimental results were analyzed with the use of the quasi-one–dimensional (quasi–1D) fluid and three–dimensional (3D) kinetic Monte Carlo codes. Numerical simulations suggest the existence of the strong fluctuation-enhanced electron diffusion and predict the non-Maxwellian shape of the electron distribution function (EDF). Through the acquired understanding of the new physics and technological challenges associated with a cylindrical geometry Hall thruster, ways for further optimization of this means for low-power space propulsion were suggested.

The investigations of the cylindrical Hall thrusters conducted at PPPL have motivated a few research projects based on the CHT concept. The performance studies of PPPL low-power cylindrical Hall thrusters were conducted at NASA Marshall Space Flight Center.[24] The experiments on cylindrical Hall thrusters are underway at Osaka University (Osaka, Japan)[25] and Korean Advanced Institute of Science and Technology (Daejeon, Korea).[26] One more thruster utilizing the CHT concept, the high efficiency multistage plasma thruster (HEMP), was developed at Thales Electron Devices (Ulm, Germany).[27,28] In terms of electron confinement and ion acceleration, HEMP is essentially a multistage cylindrical thruster.

The present paper gives a review of the experimental and numerical investigations of the CHT physics conducted at PPPL and reports a few recent experimental results that suggest directions for further studies.

This article is organized as follows: In Sec. II, the PPPL cylindrical Hall thrusters, facilities, and diagnostics are briefly described and the main features of the developed numeric models are outlined. We give an overview of the main experimental and numerical results in Sec. III, addressing the problems of propellant ionization, electron cross-field transport, ion acceleration, and plasma-wall interaction in a min-

iaturized CHT. The main conclusions are summarized in Sec. IV.

II. EXPERIMENTS AND MODELING

The CHTs with channel outer diameters of 9, 3, and 2.6 cm were built and studied at PPPL. The viability of the cylindrical Hall thruster concept was first demonstrated in the experiments with the 9-cm CHT (Ref. 15). In the present paper, the CHT physics and the observed new phenomena are discussed with the emphasis on the results obtained with the 2.6-cm CHT. The 2.6-cm CHT shown in Fig. 1(b) was scaled down from a 9-cm CHT (600–1000 W input power) to operate at about 200 W power level.

The magnetic field profiles in the 2.6-cm CHT are shown in Fig. 2. By varying the relative polarity of the currents in the thruster electromagnets, two magnetic field configurations can be generated. In the "cusp" configuration the currents in the coils are counterdirected and the radial component of the magnetic field is enhanced. When the currents have the same polarity, the axial component of the magnetic field is intensified in the cylindrical part of the channel. The typical discharge parameters for the 2.6-cm CHT are Xe flow rate $\mu=0.4$ mg/s, discharge voltage $U_d=250$ V, discharge current $I_d \approx 0.6$ A, generated ion current $I_i \approx 0.35$ A, thrust $T \approx 4$ mN. The thruster anode efficiency, which is defined as $\eta=T^2/(2\mu I_d U_d)$, varies between 25% and 40% (see Sec. III E). In this definition of efficiency the power and propellant losses associated with the operation of the cathode neutralizer are not taken into account.

The experiments were performed in the Small[16] and Large[29] Hall Thruster Facilities at PPPL, as well as in the Electric Propulsion and Plasma Dynamics Laboratory facility at the Department of Mechanical and Aerospace Engineering of Princeton University.[30] The testing facilities, diagnostics, and measurement procedures are described in detail elsewhere.[22] The angular distribution of the ion current density in the plasma stream generated by the thruster was measured by a movable electrostatic graphite probe with a guarding sleeve.[29] The distribution of plasma potential ϕ, electron temperature T_e, and plasma density N_e inside the 2.6-cm CHT and in the near-field plume was studied by means of stationary and movable, emissive and biased Langmuir probes.[31,32] Harsh environment of a Hall thruster creates significant difficulties in the collection and interpretation of Langmuir probe data. Among the numerous factors that complicate the probe measurements are probe-induced perturbations, strong magnetic field, non-Maxwellian electrons, orbital-motion-limited effects, and small thruster size. These factors were assessed and their effects on the measurements were mitigated.[22]

The Electric Propulsion and Plasma Dynamics Laboratory (EPPDyL, Princeton University) thrust stand was used for the thrust measurements. This thrust stand was designed to accurately measure impulse bits of pulsed plasma thrusters.[30] The thrust stand operation at low steady-state thrust and the accuracy of thrust measurements were investigated in detail through the comparison of several calibra-

Cusp configuration, Ifront = -1 A

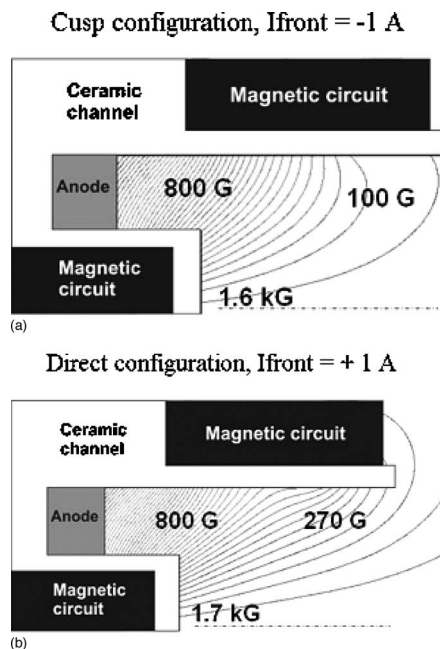Direct configuration, Ifront = + 1 A

FIG. 2. The magnetic field distribution in the channel of the 2.6-cm CHT in the (a) cusp and (b) direct configurations. The current in the back coil is fixed (I_{back}=3 A). Note that the variation of I_{front} alters the magnetic field distribution in the annular part of the channel insignificantly.

tion and measurement techniques. To decrease the experimental uncertainty, special calibration and measurement procedures were developed.[20]

Two numerical models were developed to analyze the experimental results. First, a hydrodynamic, stationary, quasi-1D Hall thruster model was developed to study the effect of the reduction of energy and particle wall losses on the Hall thruster operation.[17] The model incorporates the ion flux continuity equation and the ion momentum equation with ionization and ion wall losses taken into account. The electron distribution function is assumed to be Maxwellian. The electron motion across the magnetic field is governed by the generalized Ohm's law, which accounts for electron-neutral and electron-wall collisions, and the anomalous (Bohm) diffusion. The plasma-wall interaction in the presence of strong secondary electron emission (SEE) from the channel walls is taken into account and the space-charge saturation of the near-wall sheath[33] for realistic SEE properties is calculated self-consistently.

The 3D kinetic Monte Carlo (MC) code was developed to simulate the charged particles dynamics in the channel of the 2.6-cm CHT.[19] Specifically, the MC simulations were designed to address two physical questions: (i) What rate of electron cross-field diffusion could possibly explain the observed discharge current? (ii) How does the electron-wall interaction affect the EDF formation (see Sec. III C)? The particle trajectories are traced in the given electric and magnetic fields. The magnetic field distribution for a given arrangement of the magnetic circuit is simulated using commercially available software, while the electric field distribution is obtained from the experiments assuming that the magnetic field surfaces are equipotential. The charged particle trajectories are integrated in 3D-3v (three dimen-

sions in configuration space, three dimensions in velocity space). We apply the MC technique[34] to simulate electron collisions, which include collisions with neutral Xe atoms (elastic scattering, excitation, and single ionization), with channel walls (attachment, backscattering, and secondary electron emission), and with electric field fluctuations (see Sec. III C).

III. RESULTS

A. Ion acceleration and electron confinement

As shown in Fig. 3, in the 2.6-cm CHT, similarly to the large 9-cm cylindrical thruster,[15] a significant part of the voltage drop is localized in the cylindrical part of the channel. Since equipotentials tend to follow the magnetic field lines, a complex two-dimensional (2D) structure of the accelerating electric field is formed in the channel.[35] Ions born in the annular part of the channel should be accelerated predominantly in the z direction and towards the thruster axis. Therefore, the outer wall erosion might be decreased and a longer lifetime of the cylindrical thruster, as compared with conventional geometry Hall thrusters, could be expected.

The considerable potential drop observed along the thruster axis in the plume of the 2.6-cm CHT plays an important role in confining the electrons in the discharge. Due to the mirroring effect of the magnetic field in the cylindrical part of the channel [see Fig. 1(a)], most of the electrons injected into the thruster from the cathode are reflected from the region of strong B field, and move in the downstream direction. Upon crossing the thruster exit plane and entering the plume plasma, the electrons become unmagnetized and face the potential drop of about 100 V, which reflects them back into the thruster. Thus, most of the electrons injected from the cathode to the 2.6-cm CHT appear to be confined in a hybrid trap formed by the magnetic mirror and by the plume potential drop. Diffusion of these electrons across the magnetic field occurs on a time scale much larger than the bounce time in the trap.[19]

As can be seen in Fig. 3(b), the potential drop along the thruster axis between the central ceramic piece and the channel exit is insignificant.[36] This fact can be explained as follows. In general, for the collisionless Maxwellian electrons, the variation of the electron density along the mirror magnetic field is independent of B and follows the Boltzmann distribution,[37]

$$N_e = N_0 \exp(e\phi(x)/T_e). \tag{1}$$

Here, $\phi(x)$ is the plasma potential profile along the mirror axis, which should be found as a solution to the Poisson equation. Note that the ion density distribution, which self-consistently affects $\phi(x)$ through the Poisson equation, is independent of the magnetic field in a Hall thruster as well, because ions are not magnetized. Thus, the axial profile of the ambipolar plasma potential should not be dependent on B. However, we do expect some axial variation of the plasma potential to occur in the 2.6-cm CHT. This variation is associated with the possible ion density elevation at the thruster axis due to the ion flux focusing.[22]
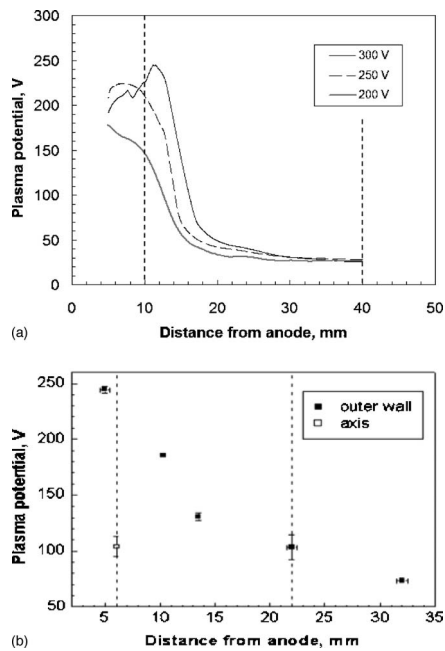
FIG. 3. (a) The axial distributions of the plasma potential in the 9-cm CHT for the discharge voltage of 300, 250, and 200 V. The fast reciprocating probe was inserted along the median of the annular part of the channel (Ref. 15). (b) The axial profile of the plasma potential in the 2.6-cm CHT for the discharge voltage of 250 V (Ref. 18). Dashed lines at (a) $z=10$ mm and $z=40$ mm, and (b) $z=6$ mm and $z=22$ mm show the edge of the annular channel part and the thruster exit, respectively.
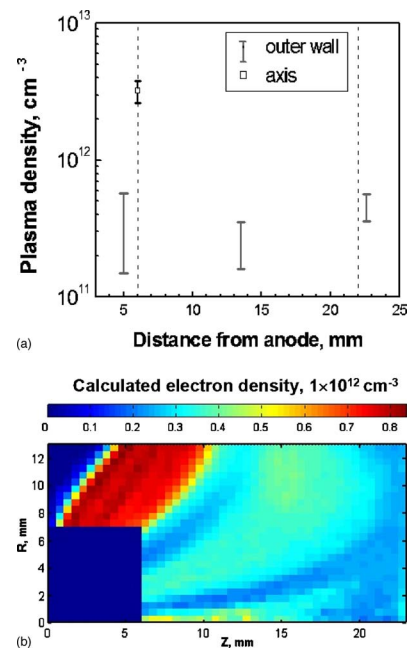

FIG. 4. (Color online) The (a) measured and (b) calculated plasma density profile in the 2.6-cm CHT (Ref. 19). For plasma density measurements, only the intervals in which the real values of the plasma density are located, can be given. Dashed lines at $z=6$ mm and $z=22$ mm show the edge of the annular channel part and the thruster exit, respectively.

The measured distribution of the plasma density N_e inside the 2.6-cm CHT is shown in Fig. 4(a). Due to a rather large uncertainty of the plasma density measurements, it was possible to determine only the interval, in which the real value of N_e was located. The variation bars in Fig. 4(a) span between the upper and lower estimates of N_e obtained in the experiments. The plasma density in the 2.6-cm CHT has a prominent peak at the thruster axis: N_e at the axis is 4–8 times larger than in the annular part of the channel. This sharp density maximum is believed to be the manifestation of the convergent ion flux.

The distribution of electron density N_e obtained in the MC simulations[19] is shown in Fig. 4(b). As opposed to the results of the experiments, the electron density at the thruster axis is lower than the density in the annular part of the channel. Note that there is no significant elevation of the electron density towards the mirror plug near the front wall of the central ceramic piece. The EDF in the near-axis region is close to isotropic, and, as argued above, in the absence of the electric field the electron density should be uniform along the mirror axis regardless of the mirror ratio of the magnetic field [see Eq. (1)]. Thus, the plasma density spike experimentally observed at the thruster axis is most likely due to the focusing of accelerated ions. This effect cannot be captured in the electron MC simulations, because our MC code uses the experimentally obtained electric field as input and does not solve for the self-consistent electric field.

In the vicinity of the geometric "focal point" of the ion flux, there should appear a self-consistent ambipolar potential peak associated with the plasma density elevation. The height of this potential peak is of the order of the electron temperature. The reflection of slow ions off the potential peak may increase the ion residence time in the plasma.[22]

B. Ionization of neutrals

Figure 5(a) displays the measured distribution of the electron temperature in the channel of the 2.6-cm CHT. With $T_e \sim 15$ eV and $N_e \sim 5 \times 10^{11}$ cm^{-3} [see Fig. 4(a)], the mean free path λ_{ni} of a neutral atom with respect to ionization by electron impact is about 0.5 cm, which is approximately equal to the length of the annular part of the channel. Thus, ionization of neutral atoms supplied through the anode occurs mainly near the boundary of the annular and cylindrical channel regions.

The ion flux measurements showed that the propellant ionization efficiency of the cylindrical thruster is much higher than that of the conventional, annular geometry thrusters.[16,22] In Fig. 5(b) the dependence of the propellant utilization on the discharge voltage is displayed for the 2.6-cm CHT and a conventional, annular geometry thruster of the same channel size. The propellant utilization η_p is defined as a ratio of the total ion current I_i at the thruster exit plane to the propellant flow rate μ measured in units of electric current. Namely, $\eta_p = I_i M / e \mu$, where M is the mass of a propellant gas atom and e is the electron charge. For any given discharge voltage and anode flow rate, the thrust generated in the cylindrical thruster is larger than that in the annular one, which is yet another indication of the fact that the ion current generated by the cylindrical thruster is larger.

Interestingly, the propellant utilization in the CHT can exceed unity, which implies a presence of xenon ions in charge states higher than +1 in the ion flux. It is important to
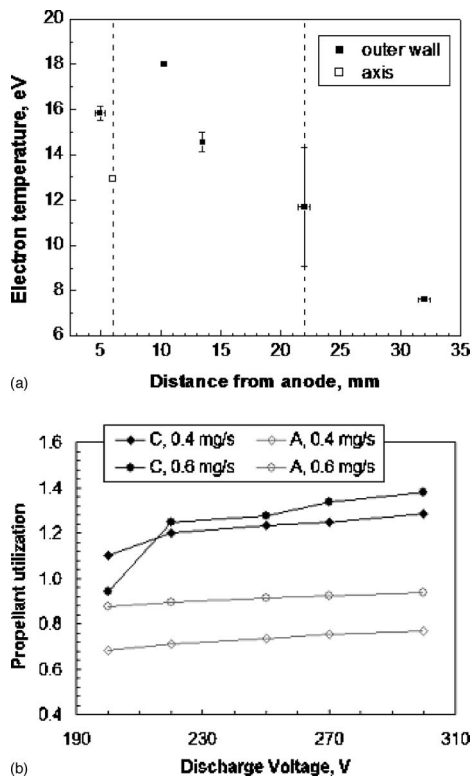
FIG. 5. (a) The electron temperature profile in the 2.6-cm CHT (Ref. 18). Dashed lines at $z=6$ mm and $z=22$ mm show the edge of the annular channel part and the thruster exit, respectively. (b) The dependence of the propellant utilization, $\eta_p = I_i M / e_\mu$, on the discharge voltage for the 2.6-cm annular thruster (A, open symbols) and cylindrical thruster in the direct magnetic configuration (C, solid symbols). The anode flow rate is varied as a parameter.

mention that the ion current density measurements in the plume were repeated several times in different facilities and great care was taken to minimize the possible effects of the background gas on the ion current. In particular, during the measurements in the low background gas pressure environment ($p_{\text{bckgr}} \sim 3 \times 10^{-6}$ Torr), the hollow cathode was replaced by an electron-emitting filament and the gas flow to the cathode was shut off. Under such conditions, the measured propellant utilization was still as large as $\eta_p \sim 1.3$. The background gas was not ionized in the plume plasma and, thus, could not account for the large values of η_p (Ref. 22).

The fact that the ion flux produced by the thruster apparently contains a substantial fraction of multicharged xenon ions is of particular interest. The quasi-1D fluid thruster model rules out the possibility that the propellant utilization enhancement is due to the decrease of the ion wall losses.[17] The major factor in multicharged ions formation in a Hall thruster is the ion residence time in the channel. Simple estimates show that in the conventional thruster geometry, where the electric field is mainly axial, the time of flight of a Xe$^+$ ion through a channel is much smaller than the time of ionization to higher charge states. For example, for $T_e \sim 20$ eV and $N_e \sim 5 \times 10^{11}$ cm^{-3} the rate coefficient for single electron impact ionization Xe$^{+1} \rightarrow$ Xe^{+2} is about $k_{1,2} \sim 2 \times 10^{-8}$ cm^3/s. Therefore, even for a moderately energetic ion with $E_i = 50$ eV, the time of flight through a channel

with length 3 cm $\tau_f \sim 4 \times 10^{-6}$ s is approximately one order of magnitude smaller than the ionization time $\tau_{1,2} \sim (N_e k_{1,2})^{-1} \sim 6 \times 10^{-5}$ s. In the case of the cylindrical thruster, the 3D MC simulations and analysis of experimental data suggest that due to the ion beam focusing in the cylindrical part of the channel, a localized peak of the ambipolar plasma potential, associated with the increase of the ion density, may appear at the thruster axis. The reflection of slow ions off the potential peak back into the thruster should increase the ion residence time in the discharge and, thereby, could help to explain the enhanced propellant utilization.

C. Anomalous electron transport

The efficiency of a Hall thruster, which is defined as $\eta = T^2/(2\mu I_d U_d)$, can be conveniently factored as

$$\eta \approx \eta_p \times \eta_V \times \frac{I_i}{I_i + I_e}, \qquad (2)$$

where η_p is the propellant utilization, η_V is the efficiency of ion acceleration, and the fraction in the right-hand side of Eq. (2), the so-called current utilization, determines how effectively the electron transport to the anode is suppressed by the applied magnetic field. With all other parameters held constant, the thruster efficiency decreases with increasing electron current. Understanding of the mechanisms of electron transport in the discharge is, therefore, essential for the development of higher efficiency thrusters. In the experiments, the electron current can be found as the difference between the discharge current and the total ion current, deduced from the measurements of the ion current density distribution in the plume. The important assumption here is that ionization and charge exchange in the plume do not significantly change the value of the ion current between the thruster exit and the measurement plane. As shown in Fig. 6, the electron current in the miniaturized cylindrical thruster is a few times larger than that in the annular thruster of the same size. The efficiency of the CHT is, however, comparable to that of the conventional geometry thruster, because of the unusually high propellant utilization (see Sec. III B).

The electrons in Hall thrusters exhibit anomalous cross-field transport: The electron conductivity across the magnetic field is larger than that predicted by the classical electron-atom collision rate.[2,38] It is generally believed that two collisional processes contribute to the conductivity enhancement in Hall thrusters: (i) electron scattering in electric field fluctuations,[38] and (ii) the electron-wall collisions (the near-wall conductivity[39,40]). In Hall discharge simulations, in order to account for the enhanced electron cross-field transport, the two nonclassical conductivity mechanisms are usually incorporated in one or another parametric way.

It is important to emphasize that most of investigations that addressed the question of the electron conductivity in $\mathbf{E} \times \mathbf{B}$ discharges have been done for Hall thrusters with the maximal magnetic field of about 100–200 G. Scaled down, low-power thrusters have much larger magnetic fields (since the magnetic field must be increased inversely to the scaling factor). Thus, in principle, the rate of electron cross-field
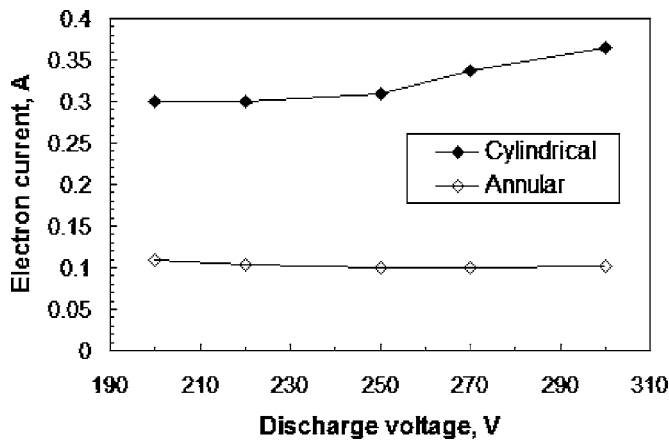
FIG. 6. The dependence of the electron current injected into the thruster, $I_e = I_d - I_i$, on the discharge voltage for the 2.6-cm cylindrical and annular thrusters. The anode flow rate is 0.4 mg/s.

FIG. 7. Calculated profiles of the plasma density at the outer channel wall for different values of κ_B. The uncertainty bars represent the results of the plasma density measurements.

transport required to sustain the discharge in a low-power thruster may be different from that in kilowatt thrusters.

The electron cross-field transport in the miniaturized cylindrical thruster was studied through the analysis of experimental data and Monte Carlo simulations of electron dynamics in the thruster channel.[19] In simulations, the frequency of anomalous electron collisions ν_B was assumed to be proportional to the Bohm diffusion frequency, $\nu_B = \kappa_B \omega_c/16$, where κ_B is a fitting parameter and ω_c is the electron gyrofrequency. As opposed to most of the conventional Hall thruster models,[41–45] which predict the ratio ν_B/ω_c to be on the order of 10^{-2}, we found that in the 2.6-cm CHT, ν_B has to be on the order of, or possibly even larger than, the Bohm value. Figure 7 shows how the calculated electron density profile changes with κ_B. In order to explain the observed discharge current and plasma density, the electron anomalous collision frequency ν_B has to be high: $\kappa_B \gtrsim 1$, which corresponds to $\nu_B \gtrsim \omega_c/16$.

The anomalous electron cross-field transport in the CHT is believed to be induced by high-frequency plasma instabilities.[46,47] The electron-wall collisions likely make an insignificant contribution to the electron current conduction, as compared with the fluctuation-induced electron scattering. The reason for this, as explained in the next section, is the depletion of the tail of the electron distribution function caused by electron-wall interaction. For the typical discharge conditions, the electron-wall and the electron-atom collision frequencies are much less than the anomalous collision frequency, which is required to explain the observed discharge current: $\nu_{ew} \sim \nu_{ea} \ll \nu_B$.

The electron transport to the anode can be suppressed and the thruster efficiency increased by optimizing the magnetic field configuration of the CHT.[22] The increase of the current in the front magnetic coil I_{front} (i.e., the enhancement of the magnetic field in the cylindrical part of the channel) brings about an increase in the thruster current utilization. Along with it, as the magnetic field configuration is changed from cusp to direct, the generated thrust slightly increases [see Fig. 8(a)]. Consequently, the CHT efficiency η_a in the direct configuration is approximately a factor of 1.5–1.7
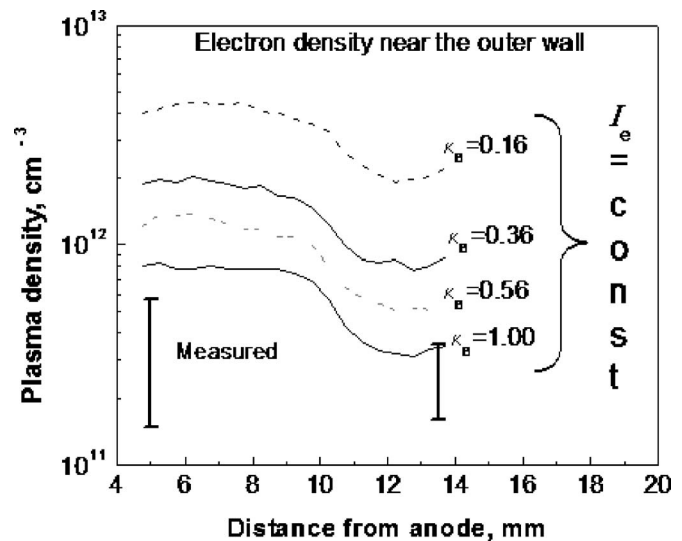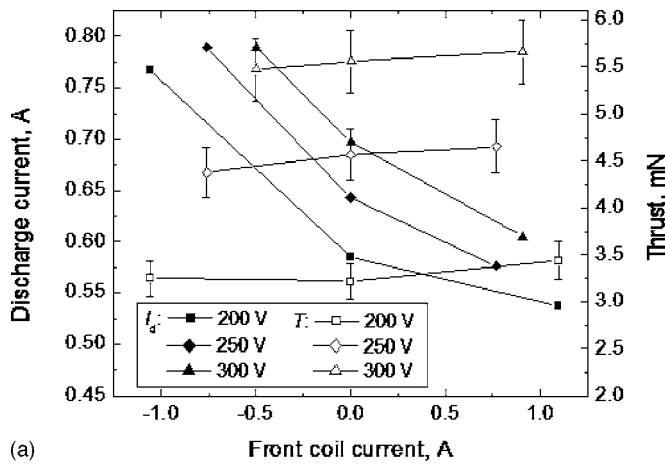
larger than that in the cusp configuration [see Fig. 8(b)]. The thruster anode efficiency reaches ~25% in the power range 100–200 W, which is comparable to the state-of-the-art, annular, low-power Hall thrusters. Note that unlike in the conventional thruster geometry, the increase of the axial component of the magnetic field in the CHT leads to the reduction of the axial electron current.

In general, the axial distributions of the plasma density, electric field, and electron temperature in the cusp and direct magnetic configurations are very similar.[22] For example, as shown in Fig. 9, the plasma potential profile is fairly insensitive to the variation of the magnetic configuration. Thus, qualitatively, the reduction of the electron current, associated with the change of the magnetic field polarity from cusp to direct, must be attributed to the suppression of the anomalous electron mobility. Under the assumption of the Bohm-like scaling for the anomalous collision frequency, from the generalized Ohm's law in the direction across the magnetic field it follows that
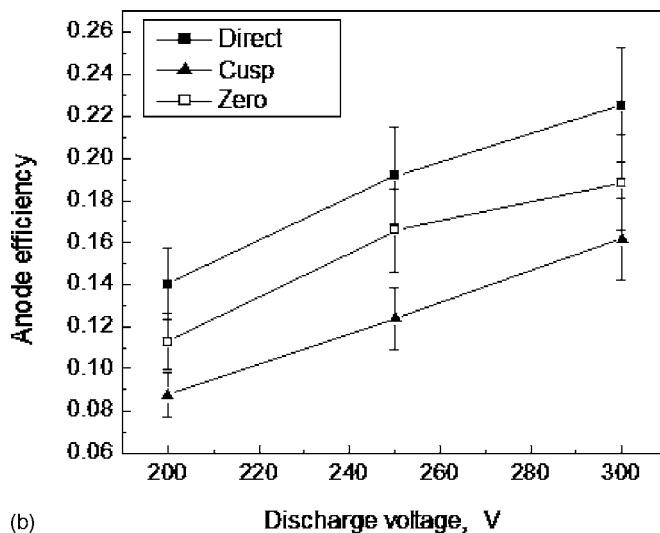
$$\kappa_B \propto \frac{j_e B}{N_e E}. \tag{3}$$

The analysis of experimental data based on Eq. (3) suggests that: (1) In the annular part of the channel, where the magnetic field is fairly insensitive to the front coil current, the rate of the anomalous diffusion in the direct configuration reduces slightly with respect to that in the cusp polarity. However, due to a relatively large uncertainty in the plasma density measurements, it is difficult to accurately quantify the ratio $\kappa_B^{dir}/\kappa_B^{cusp}$. (2) In the cylindrical part of the channel the increase of the front coil current enhances the magnetic field, which leads to the reduction of the rate of the anomalous electron cross-field transport and the effective Bohm parameter,

$$\frac{\kappa_B^{dir}}{\kappa_B^{cusp}} \propto \frac{I_e^{dir}}{I_e^{cusp}} \times \frac{\langle B \rangle^{dir}}{\langle B \rangle^{cusp}} \sim 0.5. \tag{4}$$
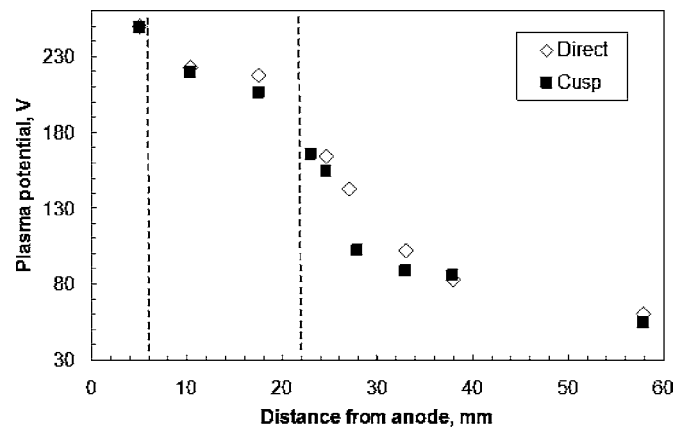
(a)

FIG. 9. The axial distributions of the plasma potential relative to the cathode for the cusp and direct magnetic configurations of the 2.6-cm CHT. The discharge parameters are $\mu=0.4$ mg/s, $V_d=250$ V, $I_{back}=+3$ A, $I_{front}=+0.95$ A (direct), -0.7 A (cusp). The dashed lines at $z=6$ mm and $z=22$ mm show the edge of the annular channel part and the thruster exit, respectively.

(b)

FIG. 8. (a) The dependencies of the discharge current and thrust on the front coil current and (b) the dependence of the anode efficiency on the discharge voltage for different magnetic configurations for the 2.6-cm CHT. $I_{back}=+3$ A. $I_{front}>0$ ($I_{front}<0$) corresponds to the direct (cusp) magnetic field configuration.

D. Plasma-wall interaction

Plasma-wall interaction in a Hall thruster affects the device performance in two ways: First, the losses of charged particles and energy at the channel walls decrease the plasma density and electron temperature and reduce the thruster efficiency. Second, electrons that scatter at the walls contribute to cross-field transport (the so-called "near-wall" conductivity[39,40]).

A commonly accepted approach in the state-of-the-art fluid models of Hall thruster operation is to assume the electron distribution function to be Maxwellian.[41,44,48–51] The conventional Hall thruster channel materials, such as boron nitride, have high secondary electron emission coefficients.[52] For typical electron temperatures of about 20 eV, the flux of secondary electrons from the wall can be comparable to the incident flux of primary electrons. For Maxwellian electrons, strong SEE in a Hall thruster brings about two effects. First, the channel wall acts as an extremely effective energy sink as the SEE coefficient γ approaches unity, $\gamma \rightarrow 1$. The electron energy losses on the wall tend to limit the electron tempera-

ture in the channel at the threshold value T^* determined by the crossover energy, $\gamma(T^*) \approx 1$. Second, SEE enhances the near-wall conductivity by increasing the electron-wall collision frequency. Electron-wall collisions make a contribution to the axial current conduction in the same fashion as collisions of electrons with heavy neutrals do.

The simulations done with the 1D fluid model revealed that the fluid approach tends to overpredict the contribution of electron-wall collisions to the cross-field transport and cannot quantitatively explain the observed electron temperature saturation in Hall thrusters. In particular, according to the fluid model, the near-wall sheath should become space-charge saturated (SCS) at $T_e \sim T^*$, where the value of T^* for boron nitride channels is about 18.3 eV (Ref. 17). However, recent experiments with the 2-kW annular Hall thruster demonstrated that the electron temperature inside a boron nitride channel was almost three times larger than the critical value predicted for the SCS sheath regime under the assumption of the Maxwellian EDF.[32,53,54] Accurate description of experimentally observed effects requires kinetic analysis of EDF formation and self-consistent treatment of electron heating, scattering, and wall losses. The electron-wall interaction plays a very important role in shaping the electron distribution function in the thruster channel.

Kinetic MC simulations of the electron dynamics in the 2.6-cm CHT showed that due to the electron attachment to the walls, the tail of the EDF appears to be depopulated. The resultant EDF shape is bi-Maxwellian, with the tail temperature a few times smaller than the bulk electron temperature. Figure 10 displays the typical EDF in the annular part of the channel, calculated for the following conditions: anode flow rate $\mu=0.4$ mg/s, $U_d=250$ V, $I_d \approx 0.6$ A, $I_e \approx 0.25$ A, $\kappa_B=1$, and the neutral gas density of 3.7×10^{13} cm^{-3} (assumed to be uniform across the entire channel). In the cylindrical part of the channel, where the electron-wall collision frequency is smaller, the influence of the walls on the EDF shape is less pronounced. The variation of the discharge voltage does not cause qualitative changes in the EDF. The
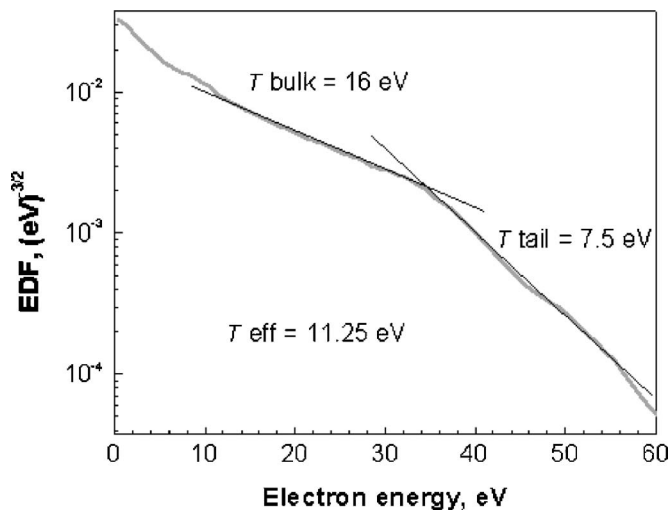
FIG. 10. The typical calculated electron distribution function (EDF) in the annular part of the 2.6-cm CHT.
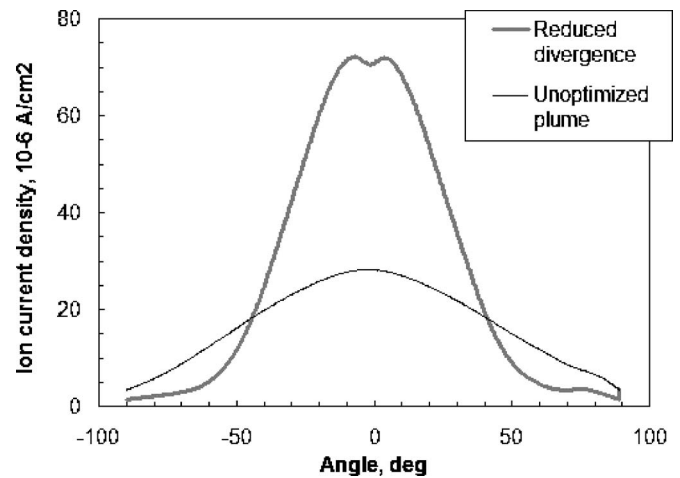

FIG. 11. (a) The angular distribution of the ion current density in the far-field plume of the 2.6-cm CHT at the input power of 160 W. The optimization of the discharge parameters results in ~30% plume angle reduction. (b) The thruster anode efficiency in the direct magnetic configuration with the usual and reduced beam divergence.

change of the magnetic field mainly affects the EDF tail depletion, because the rate at which the electrons gain thermal energy is controlled (for the given electric field) by the anomalous collision frequency ν_B (Ref. 19).

Due to the EDF tail depletion, the amount of primary electrons that can penetrate the sheath and reach the wall is small, and the contribution of electron-wall scattering to cross-field transport is likely insignificant. Note that the EDF depletion at high energy is by no means peculiar for the cylindrical thruster design only. In fact, other authors, using different theoretical approaches and numerical methods, obtained a similar effect of the plasma-wall interaction for the conventional Hall thrusters.[55–57]

E. Reduction of the beam divergence in the cylindrical Hall thruster

An unusually large beam divergence of the plasma plume has been the key drawback of existing cylindrical Hall thrusters. The plasma plume angle, θ_p, is customarily defined as the angle that contains 90% of the total ion current. In the cylindrical thrusters, the half plume angle $\theta_p/2$ can be as large as $70°–80°$ (compared to $45°–50°$ for the state-of-the-art annular HTs). Since the CHT has possibly stronger radial electric field than the conventional HT, more energetic ions may escape at large angles with respect to the thruster axis. Very recently,[58] a dramatic reduction of the plume angle in the 2.6-cm CHT was achieved as a result of the optimization of the magnetic circuit and discharge parameters (see Fig. 11). At the operating power of 160 W, the half plume angle was reduced to $55°$, which is comparable to the state-of-the-art conventional HTs. If the ion acceleration does not deteriorate as the plume is narrowed, the thruster anode efficiency in the direct magnetic configuration (i.e., with the suppressed electron transport) might reach 35–40% in the power range 100–200 W. The preliminary results of thrust measurements and ion energy distribution measurements in the plume indicate that the efficiency indeed increases. Figure 12 shows the results of the ion energy distribution measurements in the plume. The narrowing of the plume is accompanied by the increase of the average energy and the number of energetic ions at the thruster symmetry axis [Fig. 12(a)]. At the same time, the number of high-energy ions flying at large angles to the axis decreases [Fig. 12(b)]. Integrated over the azimuthal angle, such a change in the distribution of the ion current density and average ion energy leads to the increase of the thrust.

IV. CONCLUSIONS

Scaling to low-power Hall thrusters requires the magnetic field to be increased inversely with length, as the thruster channel size is decreased. The conventional (annular) Hall thrusters become inefficient when scaled to small sizes because of the large surface-to-volume ratio and the difficulty in miniaturizing the magnetic circuit. Also, the erosion of the walls of a small annular channel can severely limit the thruster lifetime. An alternative approach, which may be more suitable for scaling to low power, is a cylindrical Hall thruster. The 9-cm CHT, operated in the subkilowatt power range, and the miniature 2.6- and 3-cm CHT, operated in the power range 50–300 W, exhibit performance comparable with the conventional state-of-the-art annular Hall thrusters of the same size.

A comprehensive experimental and theoretical study of the physics of the low-pressure $\mathbf{E}\times\mathbf{B}$ plasma discharge in a cylindrical geometry Hall thruster was conducted, addressing the questions of potential distribution, propellant ionization, electron cross-field transport, plasma-wall interaction, and formation of the electron distribution function. The cylindrical Hall thruster differs importantly from a conventional thruster in that electrons in the cylindrical design provide charge neutralization not by not moving axially, but through being trapped axially in a hybrid magnetoelectrostatic trap. Accordingly, the underlying physics of this configuration is quite new. From the practical standpoint, CHTs, having
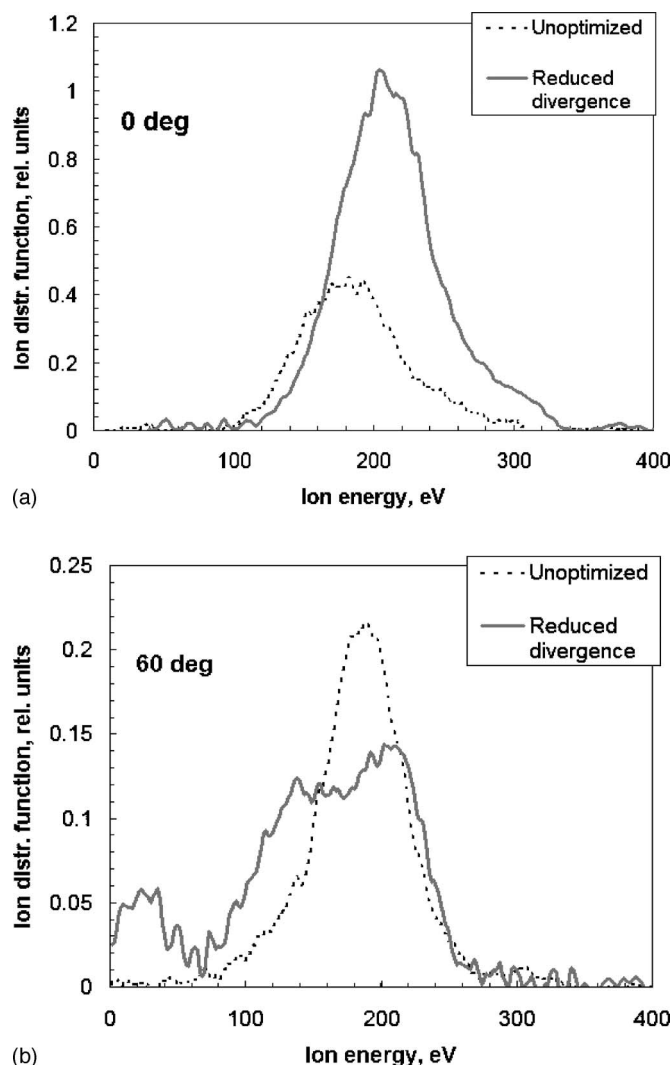
FIG. 12. The ion energy distribution function in the plume at the thruster symmetry axis (a) and at 60° off axis (b). The discharge voltage is 250 V.

bility that the propellant utilization enhancement is due to the decrease of the ion wall losses. The 3D Monte Carlo simulations and analysis of experimental data suggest that due to the ion beam focusing in the cylindrical part of the channel, a localized peak of the ambipolar plasma potential, associated with the increase of the ion density, may appear at the thruster axis. The reflection of slow ions off the potential peak back into the thruster should increase the ion residence time in the discharge and, thereby, could help to explain the enhanced propellant utilization.

The 2.6-cm CHT exhibits enhanced electron transport across the magnetic field. In order to explain the observed discharge current, the electron anomalous collision frequency ν_B has to be high. As opposed to most of the conventional Hall thruster models, which predict the ratio ν_B/ω_c to be on the order of 10^{-2}, we find that in the 2.6-cm CHT ν_B has to be on the order of, or possibly even larger than, the Bohm value, $\nu_B \gtrsim \omega_c/16$. The anomalous cross-field electron transport in the CHT is believed to be induced by high-frequency plasma instabilities. Interestingly, in the frequency range below $\sim$100 kHz, the 2.6-cm CHT operates quieter than the annular Hall thrusters of the same size.

It was demonstrated that the electron transport to the anode can be suppressed and the thruster efficiency increased by optimizing the magnetic field configuration of the CHT. The enhancement of the magnetic field in the cylindrical part of the channel leads to about a twofold decrease in ν_B/ω_c and a slight increase of the generated thrust. Accordingly, the electron current becomes smaller and the thruster efficiency larger.

The kinetic Monte Carlo simulations of the formation of the electron distribution function in a Hall thruster discharge were performed, with particular attention paid to the effects of electron heating and scattering, secondary electron emission, and wall losses. The simulations indicated that the EDF in a Hall thruster is depleted at high energy due to the electron attachment to the walls. This result helps to explain the observed reduced sensitivity of Hall thruster operation to secondary electron emission from the channel walls and implies that the contribution of electron-wall scattering to cross-field transport in the 2.6-cm CHT is likely insignificant.

Finally, a substantial reduction of the beam divergence was achieved by optimizing the magnetic field distribution and discharge parameters. The thruster plume angle was narrowed to the values comparable with those of the conventional annular Hall thrusters ($\theta_p/2 \sim 55°$). The preliminary thrust measurements indicate that in the power range 100–200 W it might be possible to increase the thruster anode efficiency from $\sim$25%, which is typical for the direct magnetic configuration (i.e., with the suppressed electron transport), to $\sim$35–40%. Thus, the miniaturized CHT, having potentially longer lifetime than conventional geometry Hall thrusters of similar size, appears promising for low-power space propulsion.

lower surface-to-volume ratio than conventional thrusters, seem to be more promising for scaling to low power and small size.

The plasma probe measurements in the CHT demonstrated that the applied voltage drop is localized mainly in the cylindrical part of the channel and in the plume. Thus, ion acceleration occurs predominantly in the longitudinal direction and towards the thruster axis in the channel region that has small area of the walls exposed to the plasma. Therefore, the CHT should suffer less erosion of the channel due to fast ion bombardment than the conventional geometry thrusters. This is particularly important for the low-power Hall thruster scaling, because the channel erosion is the factor that severely limits the lifetime of currently existing annular low-power Hall thrusters.

The ion flux and thrust measurements showed that the propellant ionization efficiency of the cylindrical thruster is much higher than that of the conventional, annular geometry thrusters. In the cylindrical thruster, a significant fraction of multicharged xenon ions can be present in the outgoing ion flux. The quasi-1D fluid thruster model rules out the possi-

[1] R. G. Jahn, *Physics of Electric Propulsion* (McGraw-Hill, New York, 1968), p. 142.

[2] A. I. Morozov and V. V. Savelyev, in *Review of Plasma Physics*, edited by B. B. Kadomtsev and V. D. Shafranov (Consultants Bureau, New York, 2000), Vol. 21, p. 203.

[3] V. V. Zhurin, H. R. Kaufman, and R. S. Robinson, Plasma Sources Sci. Technol. **8**, 1 (1999).

[4] S. W. Janson, *Proceedings of the 29th Joint Propulsion Conference and Exhibit, Monterey, CA, June 1993* (American Institute of Aeronautics and Astronautics, Reston, VA, 1993), AIAA Paper No. 1993-2220.

[5] R. R. Hofer, Ph.D. dissertation, University of Michigan, 2004.

[6] J. Mueller, in *Micropropulsion for Small Spacecraft, Progress in Astronautics and Aeronautics*, edited by M. M. Micci and A. D. Ketsdever (American Institute of Aeronautics and Astronautics, Reston, VA, 2000), Vol. 187, p. 45.

[7] S. Janson, *Proceedings of the Formation Flying and Micro-Propulsion Workshop, Lancaster, CA, October 1998* (Air Force Research Laboratory, Lancaster, CA, 1998), p. 5.

[8] F. S. Gulczinski III, M. J. Dulligan, J. P. Lake, and G. G. Spanjers, *Proceedings of the 36th Joint Propulsion Conference, Huntsville, AL, July 2000* (American Institute of Aeronautics and Astronautics, Reston, VA, 2000), AIAA Paper No. 2000-3255.

[9] M. Martin and M. J. Stallard, *Proceedings of the AIAA Space Technology Conference, Albuquerque, NM, September 1999* (American Institute of Aeronautics and Astronautics, Reston, VA, 1999), AIAA Paper No. 1999-4479.

[10] P. Stephens, J. Cooksley, A. Da Silva Curiel, *Proceedings of the International Conference on Recent Advances in Space Technologies, Istanbul, Turkey, 20–22 November 2003* (Institute of Electrical and Electronics Engineers, Piscataway, NJ, 2003), p. 525.

[11] R. L. Ticker and D. McLennan, *Proceedings of the IEEE Aerospace Conference, Big Sky, MT, March 2000* (Institute of Electrical and Electronics Engineers, Piscataway, NJ, 2000), Vol. 7, p. 609.

[12] J. Ashkenazy, Y. Raitses, and G. Appelbaum, *Proceedings of the 2nd European Spacecraft Propulsion Conference, Noordwijk, The Netherlands, May 1997* (European Space Agency, Noordwijk, The Netherlands, 1997), Paper No. ESA SP-398.

[13] C. Clauss, M. Day, V. Kim, Y. Kondakov, and T. Randolph, *Proceedings of the 33rd Joint Propulsion Conference, Seattle, WA, July 1997* (American Institute of Aeronautics and Astronautics, Reston, VA, 2000), AIAA Paper No. 1997-2789.

[14] V. Khayms and M. Martinez-Sanchez, in *Micropropulsion for Small Spacecraft, Progress in Astronautics and Aeronautics*, edited by M. M. Micci and A. D. Ketsdever (American Institute of Aeronautics and Astronautics, Reston, VA, 2000), Vol. 147, p. 233.

[15] Y. Raitses and N. J. Fisch, Phys. Plasmas **8**, 2579 (2001).

[16] A. Smirnov, Y. Raitses, and N. J. Fisch, J. Appl. Phys. **92**, 5673 (2002).

[17] A. Smirnov, Y. Raitses, and N. J. Fisch, J. Appl. Phys. **94**, 852 (2003).

[18] A. Smirnov, Y. Raitses, and N. J. Fisch, J. Appl. Phys. **95**, 2283 (2004).

[19] A. Smirnov, Y. Raitses, and N. J. Fisch, Phys. Plasmas **11**, 4922 (2004).

[20] A. Smirnov, Y. Raitses, and N. J. Fisch, *Proceedings of the 29th International Electric Propulsion Conference, Princeton, NJ, 2005* (Electric Rocket Propulsion Society, Cleveland, OH, 2005), IEPC Paper No. 2005-099.

[21] A. Smirnov, Y. Raitses, and N. J. Fisch, IEEE Trans. Plasma Sci. **34**, 132 (2006).

[22] A. Smirnov, Ph.D. dissertation, Princeton University, 2006.

[23] H. R. Kaufman, R. S. Robinson, and R. I. Seddon, J. Vac. Sci. Technol. A **5**, 2081 (1987).

[24] K. A. Polzin, T. E. Markusic, B. J. Stanojev, A. Dehoyos, Y. Raitses, A. Smirnov, and N. J. Fisch, *Proceedings of the 29th International Electric Propulsion Conference, Princeton, NJ, 2005* (Electric Rocket Propulsion Society, Cleveland, OH, 2005), IEPC Paper No. 2005-011.

[25] A. Shirasaki and H. Tahara, *Proceedings of the 29th International Electric Propulsion Conference, Princeton, NJ, 2005* (Electric Rocket Propulsion Society, Cleveland, OH, 2005), IEPC Paper No. 2005-051; see also, A. Shirasaki, H. Tahara, and T. Yoshikawa, *Proceedings of the 28th International Electric Propulsion Conference, Toulouse, France, March 2003* (Electric Rocket Propulsion Society, Cleveland, OH, 2003), IEPC Paper No. 2003-51.

[26] J. Lee, W. Choe, and K. Chai, in *Bulletin of the Korean Physics Society, Proceedings of the 82nd Meeting of the Korean Physics Society, Pyung Chang, Korea, April 2006* (Korean Physics Society, Pyung Chang, 2006), Paper No. Hp3-060.

[27] N. Koch, H.-P. Harmann, and G. Kornfeld, *Proceedings of the 29th International Electric Propulsion Conference, Princeton, NJ, 2005* (Electric Rocket Propulsion Society, Cleveland, OH, 2005), IEPC Paper No. 2005-297.

[28] G. Kornfeld, N. Koch, and G. Coustou, *Proceedings of the 28th International Electric Propulsion Conference, Toulouse, France, March 2003* (Electric Rocket Propulsion Society, Cleveland, OH, 2003), IEPC Paper No. 2003-212.

[29] Y. Raitses, D. Staack, A. Dunaevsky, L. Dorf, and N. J. Fisch, *Proceedings of the 28th International Electric Propulsion Conference, Toulouse, France, March 2003* (Electric Rocket Propulsion Society, Cleveland, OH, 2003), IEPC Paper No. 2003-0139.

[30] E. A. Cubbin, J. K. Ziemer, E. Y. Choueiri, R. G. Jahn, Rev. Sci. Instrum. **68**, 2339 (1997).

[31] D. Staack, Y. Raitses, and N. J. Fisch, Rev. Sci. Instrum. **75**, 393 (2004).

[32] Y. Raitses, D. Staack, A. Smirnov, and N. J. Fisch, Phys. Plasmas **12**, 073507 (2005).

[33] G. D. Hobbs and J. A. Wesson, Plasma Phys. **9**, 85 (1967).

[34] C. K. Birdsall, IEEE Trans. Plasma Sci. **19**, 65 (1991).

[35] The focusing effect of a plasma lens is also used in the conventional geometry Hall thrusters. See, for example, A. I. Morozov and V. V. Savelyev, in *Review of Plasma Physics*, edited by B. B. Kadomtsev and V. D. Shafranov. (Consultants Bureau, New York, 2000), Vol. 21, p. 203; R. R. Hofer, Ph.D. dissertation, University of Michigan, 2004; A. Fruchtman and A. Cohen-Zur, Appl. Phys. Lett. **89**, 111501 (2006).

[36] Much larger potential drops along the magnetic field lines were observed in the Kaufman end-Hall ion source [H. R. Kaufman, R. S. Robinson, and R. I. Seddon, J. Vac. Sci. Technol. A **5**, 2081 (1987)], which has a mirror-type magnetic field distribution similar to that in the central part of the CHT.

[37] A. V. Turlapov and V. E. Semenov Phys. Rev. E **57**, 5937 (2001).

[38] G. S. Janes and R. S. Lowder, Phys. Fluids **9**, 1115 (1966).

[39] A. I. Bugrova, A. I. Morozov, and V. K. Kharchevnikov, Sov. J. Plasma Phys. **16**, 849 (1990).

[40] A. I. Morozov and V. V. Savel'ev, Plasma Phys. Rep. **27**, 570 (2001).

[41] E. Ahedo, J. M. Gallardo, and M. Martinez-Sanchez, Phys. Plasmas **10**, 3397 (2003).

[42] A. Cohen-Zur, A. Fruchtman, J. Ashkenazy, and A. Gany, Phys. Plasmas **10**, 4363 (2002).

[43] J. M. Fife, Ph.D. thesis, Massachusetts Institute of Technology, 1998.

[44] M. Keidar, I. D. Boyd, and I. I. Beilis, Phys. Plasmas **8**, 5315 (2001).

[45] J. J. Szabo, Ph.D. thesis, Massachusetts Institute of Technology, 2001.

[46] E. Y. Choueiri, Phys. Plasmas **8**, 1411 (2001).

[47] A. A. Litvak, Y. Raitses, and N. J. Fisch. Phys. Plasmas **11**, 1701 (2004); see also, A. A. Litvak and N. J. Fisch. Phys. Plasmas **11**, 1379 (2004).

[48] J. Bareilles, G. J. M. Hagelaar, L. Garrigues, C. Boniface, J. P. Boeuf, and N. Gascon, Phys. Plasmas **11**, 3035 (2004).

[49] S. Barral, K. Makowski, Z. Peradzynski, N. Gascon, and M. Dudeck, Phys. Plasmas **10**, 4137 (2003).

[50] J. P. Boeuf, and L. Carrigues. J. Appl. Phys. **84**, 3541 (1998).

[51] L. Dorf, V. Semenov, and Y. Raitses, Appl. Phys. Lett. **83**, 2551 (2003).

[52] A. Dunaevsky, Y. Raitses, and N. J. Fisch, Phys. Plasmas **10**, 2574 (2003).

[53] D. Staack, Y. Raitses, and N. J. Fisch, Appl. Phys. Lett. **84**, 3028 (2004).

[54] Y. Raitses, D. Staack, M. Keidar, and N. J. Fisch, Phys. Plasmas **12**, 057104 (2005).

[55] N. B. Meezan and M. A. Cappelli, Phys. Rev. E **66**, 036401 (2002).

[56]D. Sydorenko, A. Smolyakov, I. Kaganovich, and Y. Raitses, Phys. Plasmas **13**, 014501 (2006).

[57]I. D. Kaganovich, Y. Raitses, D. Sydorenko, and A. Smolyakov, Phys. Plasmas **14**, 057104 (2007).

[58]Y. Raitses, A. Smirnov, and N. J. Fisch, *Proceedings of the 37th AIAA Plasmadynamics and Lasers Conference, San Francisco, CA, 2006* (American Institute of Aeronautics and Astronautics, Reston, VA, 2006), AIAA Paper No. 2006-3245.